

**The Search for Higgs Boson Production in Association
with a Top-Quark Pair in pp Collisions at $\sqrt{s} = 8$ TeV in
the Lepton Plus Jets Final State**

John Garland Wood

Charlottesville, VA

B.S., The University of California, Berkeley, 2008

A Dissertation presented to the Graduate Faculty
of the University of Virginia in Candidacy for the Degree of
Doctor of Philosophy

Department of Physics

University of Virginia

May, 2015

Abstract

The most important goal of the Large Hadron Collider (LHC) is to elucidate the mechanism of electroweak symmetry breaking. The Standard Model (SM) Higgs boson is thought to be a prime candidate for this. The newly discovered boson announced on July 4th, 2012, with a mass of $\sim 125 \text{ GeV}/c^2$, has so far been shown to be consistent with a SM Higgs. However, the final confirmation of this new particle as the SM Higgs depends on subsequent measurements of all of its properties. The observation of this new particle in association with top-quark pairs would allow the couplings of this particle to top and bottom quarks to be directly measured. $t\bar{t}H$, with Higgs decaying to $b\bar{b}$ is an excellent channel to explore due to the dominant branching ratio of Higgs to $b\bar{b}$ and the kinematic handle the $t\bar{t}$ system offers on the event. However, it presents a plethora of difficult challenges due to a low signal to background ratio and uncertainties on kinematically similar SM backgrounds. This work discusses the search for Higgs boson production in association with a top-quark pair in pp collisions at $\sqrt{s} = 8 \text{ TeV}$, collected by the Compact Muon Solenoid (CMS) experiment at the LHC. The search has been performed and published in two stages. The first analysis used the first 5.1 fb^{-1} , and was followed up by the second analysis with the full 2012 dataset, using a total integrated luminosity of 19.5 fb^{-1} .

We approve the dissertation of John Garland Wood.

Date of Signature

Supervisor: Dr. Christopher Neu

Committee Chair: Dr. Bradley Cox

Committee Member: Dr. Hank Thacker

PhD Committee Chair: Dr. Astronomy Person

Contents

| | |
|---|------------|
| Contents | iv |
| List of Figures | vi |
| List of Tables | vii |
| 1 Introduction | 1 |
| 2 Theoretical Background | 4 |
| 2.1 An Overview of Quantum Field Theory | 4 |
| 2.2 Abelian Gauge Theories of Particle Interactions | 7 |
| 2.3 Non-Abelian Gauge Theories of Particle Interactions | 9 |
| 2.4 The Higgs Mechanism in an Abelian Theory | 12 |
| 2.5 The Higgs Mechanism in a non-Abelian Theory | 14 |
| 2.6 Glashow Weinberg Salam Theory | 16 |
| 2.7 The Standard Model of Particle Physics | 22 |
| 2.8 Higgs Production in pp Collisions at the LHC | 24 |
| 2.9 $t\bar{t}H$ Production and Background Processes in pp Collisions at the LHC | 25 |
| 2.10 Potential BSM Effects on $t\bar{t}H$ production | 26 |
| 3 The Large Hadron Collider | 27 |
| 3.1 From a bottle of Hydrogen | 27 |
| 3.2 Klystron | 27 |
| 3.3 Something Comes Next | 27 |
| 3.4 The Main Injector | 27 |
| 3.5 The LHC Ring | 27 |
| 3.6 Final Structure and Beam Spacing | 28 |
| 4 The Compact Muon Solenoid | 29 |
| 4.1 The Inner Tracker | 29 |

| | | |
|----------|--|-----------|
| 4.2 | The Electromagnetic Calorimeter | 29 |
| 4.2.1 | Vacuum Photo-Triodes | 29 |
| 4.2.2 | Test Rig at UVa | 29 |
| 4.2.3 | Results of UVa Tests | 29 |
| 4.3 | The Hadronic Calorimeter | 29 |
| 4.4 | Forward Calorimetry | 30 |
| 4.5 | Magnet and Return Yoke | 30 |
| 4.6 | Muon Chambers | 30 |
| 4.7 | Data Collection Overview | 30 |
| 5 | Particle Reconstruction at CMS | 31 |
| 5.1 | Muon Reconstruction | 31 |
| 5.2 | Electron Reconstruction | 31 |
| 5.3 | Photon Reconstruction | 31 |
| 5.4 | Jet Reconstruction | 31 |
| 5.5 | Tau Reconstruction | 32 |
| 5.6 | Missing Transverse Energy Reconstruction | 32 |
| | Bibliography | 33 |
| | List of Acronyms | 36 |

List of Figures

| | | |
|-----|---|----|
| 1.1 | The CMS experiment has observed a new boson at $m \sim 125 \text{ GeV}/c^2$ | 1 |
| 1.2 | A Feynman diagram of the $t\bar{t}H$ process, with Higgs $\rightarrow b\bar{b}$, and the $t\bar{t}$ -system decaying semi-leptonically | 3 |
| 2.1 | Leading and Next to Leading Order Feynman diagrams for the coulomb scattering process | 6 |
| 2.2 | The global average of α_s , the QCD coupling constant. | 7 |
| 2.3 | A visual representation of the Higgs potential | 12 |
| 2.4 | Experimental results of the width of Z boson from LEP, comparing the hypotheses of 2, 3, or 4 neutrino generations | 24 |
| 2.5 | Recent experimental results of the top mass from the CDF detector at the Tevatron | 24 |
| 2.6 | Recent experimental results of the Higgs mass from the CMS detector at the LHC | 25 |
| 2.7 | Higgs production cross-sections at the LHC, for 7-14 TeV pp collisions | 25 |
| 2.8 | Feynman diagrams for the three largest Higgs production modes at the LHC . . | 26 |

List of Tables

| | | |
|-----|--|----|
| 2.1 | The quantum numbers Isospin and Hypercharge are assigned for each of the $SU(2)$ and $U(1)$ symmetries respectively | 20 |
|-----|--|----|

Chapter 1

Introduction

On July 4th, 2012, the Compact Muon Solenoid (CMS) and A Toroidal LHC Apparatus (ATLAS) experiments announced the discovery of a new boson of mass $\sim 125 \text{ GeV}/c^2$ [1] [2]. The particle has been shown to be increasingly consistent with the description of the boson predicted by the Higgs mechanism of the SM, as measurements on its mass, width, and quantum numbers are completed. However, there are several properties of this new boson, which remain to be tested. Figure 1.1 shows a consistent mass peak between the $H \rightarrow ZZ$ and $H \rightarrow \gamma\gamma$ channels at the CMS experiment.

The Yukawaka coupling of the Higgs boson to the top-quark in the SM is the largest coupling among the fundamental particles and is well predicted - thus offering an excellent test of the nature of the coupling of the Higgs to fermions, as well as a potential probe into physics Beyond the Standard Model (BSM) that would alter this value from the SM prediction. The production of the Higgs boson in association with top-quark pairs is the best production mode at the LHC that offers direct access to the top-Higgs coupling. The dominant production mode of Higgs at the LHC, gluon-gluon fusion, involves a triangle loop of strongly-coupled fermions, which

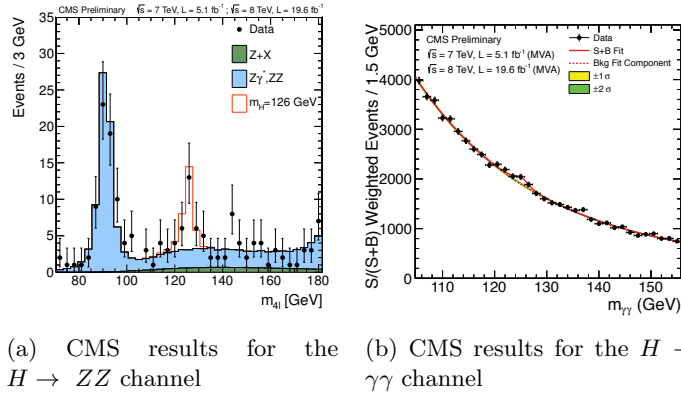


Figure 1.1: The CMS experiment has observed a new boson at $m \sim 125 \text{ GeV}/c^2$

includes all of the other quarks, as well as the potential for BSM particles.

$t\bar{t}H$ production also has the ability to constrain some extensions of the SM that would not modify the Higgs branching fractions enough to be seen within current experimental precision. Such models include Little Higgs models, models with extra dimensions, top-color models, and composite Higgs models that introduce a vector-like top partner, a t' , that can decay to tH , bW , or tZ states. Both $t't'$ and $t't$ production would produce a $t\bar{t}H$ final state, or one that is indistinguishable from it ($tHbW$). Upper limits on $t\bar{t}H$ production would also provide limits on the previously described models, which would be complementary to existing direct searches for t' particles, which attempt to reconstruct the t' resonance.

The $t\bar{t}H$ channel has a rich set of possible final states. Each top-quark will decay to a b -quark and a W boson. The W boson will subsequently decay to two quarks, or a lepton and a neutrino. These decays are classified as either hadronic, semi-leptonic, or di-leptonic for zero, one, or both t quarks decaying leptonically respectively. The Higgs may decay to b -quark, W , Z , τ , or γ pairs. In fact, this is one of the only production modes at the LHC which has access to every Higgs decay mode, as other production mechanisms are swamped by large backgrounds preventing measurements of all Higgs decay types.

The search is performed with the CMS experiment, a modern, general purpose particle detector capable of reconstructing and identifying hadronic jets, photons, electrons, muons, and tau leptons. The hermetic design, and its high precision and efficiency in reconstructing and tracking every particle in a pp collision, also makes it suitable for reconstructing missing transverse energy from the calculated momentum imbalance of all of the measured particles in the event. This missing transverse energy is often the signature of a neutrino, which is the only SM particle capable of escaping detection. The detector uses a 3.8 T axial magnetic field, produced by the solenoid it is named after, to bend charged particles as they travel through the detector. The measured curvature of their tracks allows the momentum of the particles to be calculated with to a high precision. Tracks are formed and particles are reconstructed by a combination of sub-detector systems which work together to form the final final reconstructed image of each particle in the collision.

This thesis will focus on a semi-leptonic decay of the top-quarks, with the Higgs decaying to a b -quark pair. Figure 1.2 is Feynman diagram of the $t\bar{t}H$ process. The largest background to this process is top-quark pair production with extra jets originating from Initial State Radiation (ISR) or Final State Radiation (FSR) radiation, $t\bar{t} + jets$. The irreducible background is formed by top-quark pairs, where a gluon is radiated and decays to b -quark pairs, $t\bar{t} + b\bar{b}$. In addition to the large backgrounds, the high jet multiplicity in the $t\bar{t}H$ final state gives rise to a combinatorics problem in associating each jet with its role in the $t\bar{t}H$ system. This inevitably leads to

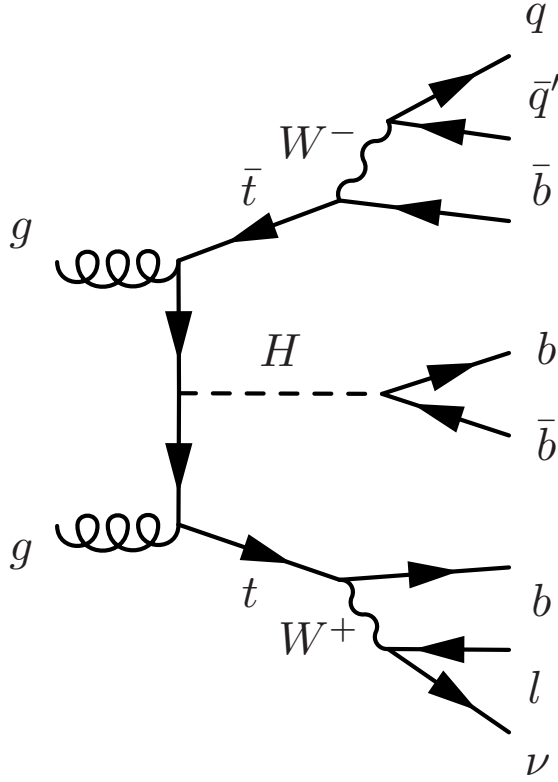


Figure 1.2: A Feynman diagram of the $t\bar{t}H$ process, with $H \rightarrow b\bar{b}$, and the $t\bar{t}$ -system decaying semi-leptonically

52 misidentifying which jets are the decay product of the Higgs, and thus additionally smears out
 53 the resolution on the mass of the Higgs. Due to the similarity of the $t\bar{t} + b\bar{b}$ background and the
 54 combinatorics issue, no single variable is suitable for signal extraction. A Multi-Variate Analysis
 55 (MVA) technique is used in an attempt to isolate the $t\bar{t}H$ signal from the $t\bar{t} + jets$ background.
 56 The MVA provides a one-dimensional discriminant based on several input variables related to
 57 the kinematics of the event. This discriminant is then used to perform signal extraction and set
 58 upper-limits on $t\bar{t}H$ production. The results of two searches will be presented. The first result
 59 used the first 5.1 fb^{-1} of the 2012 dataset, with center of mass energy of 8 TeV, and was pub-
 60 lished in the Journal of High Energy Physics (JHEP), May 2013. The second result was update
 61 with the full 19.4 fb^{-1} 8 TeV dataset, and was published in JHEP, September 2014.

Chapter 2

Theoretical Background

The Standard Model (SM) of particle physics represents the sum of knowledge of the fundamental particles and their interactions with each other. It is a Quantum Field Theory (QFT) that represents the interactions of each of the fundamental forces through the symmetry of a mathematical object known as a Lie group. It is the theory that dictates the rate that the $t\bar{t}H$ process is produced, as well as the kinematics of every particle involved. As such, its predictions are critical for modeling the characteristic signature of the $t\bar{t}H$ signal in the CMS detector, as well as the background processes, like $t\bar{t} + b\bar{b}$ which leave a kinematically similar final state signature.

2.1 An Overview of Quantum Field Theory

Quantum Field Theory (QFT) was developed out of the need for a relativistic description of quantum mechanics. Since the Einstein relation $E = mc^2$ allows for the creation of particle-antiparticle pairs, the single-particle description used in non-relativistic quantum mechanics, fails to describe this phenomenon [3]. This additionally fails when considering that Heisenberg's uncertainty relation, $\Delta E \cdot \Delta t = \hbar$, allows for an arbitrary number of intermediate, virtual particles to be created. By quantizing a field representing a certain type of particle, multiparticle states are naturally described as discrete excitations of that field.

Lorentz invariance, and the need to preserve causality, also define a fundamental relationship between matter and antimatter. The propagation of a particle across a space-like interval is treated equivalently to the an anti-particle propagating in the opposite direction [3]. This is done so that the net probability amplitude for the particles to have an effect on a measurement occurring across a space-like interval cancel each other, thus preserving causality. This cancellation requirement additionally implies that the particle and anti-particle have the same mass, with opposite quantum numbers such as spin or electric charge.

86 The Lorentz transformations for a scalar field are different than for a field with internal de-
 87 grees of freedom, such as spin. A rotation on a vector field, will affect both its location, as well
 88 as it's orientation [3]. This means the Lorentz invariant equation of motion describing a scalar
 89 field will have a different form than equations of motion for a field with spin. The most relevant
 90 equations describe the particles of SM, which contain spins of 0, 1/2, and 1. They are described
 91 by the Klein-Gordon, Dirac, and Proca equations respectively.

92

Klein-Gordon equation, for scalar (spin 0) fields

$$(\partial^2 + m^2)\phi = 0 \quad (2.1)$$

Dirac equation, for spinor (spin 1/2) fields

$$(i\gamma^\mu \partial_\mu - m)\psi = 0 \quad (2.2)$$

Proca equation, for vector (spin 1) fields

$$\partial_\mu(\partial^\mu A^\nu - \partial^\nu A^\mu) + m^2 A^\nu = 0 \quad (2.3)$$

93 With these equations, one can build a theory of free particles. The Lagrangian formulation is
 94 the most appropriate since all expressions are explicitly Lorentz invariant [3]. The Lagrangians
 95 for the Klein-Gordon, Dirac, and Proca equations are given as:

96

Klein-Gordon Lagrangian, for real and complex scalar fields

$$\begin{aligned} \mathcal{L} &= \partial_\mu \partial^\mu \phi^2 - \frac{1}{2} m^2 \phi^2 \\ \mathcal{L} &= (\partial_\mu \phi)^* (\partial^\mu \phi) - m^2 (\phi)^* (\phi) \end{aligned} \quad (2.4)$$

Dirac Lagrangian, for spinor fields

$$\mathcal{L} = i\bar{\psi}\gamma^\mu \partial_\mu \psi - m\bar{\psi}\psi \quad (2.5)$$

Proca Lagrangian, for vector fields

$$\mathcal{L} = -\frac{1}{4} F_{\mu\nu} F^{\mu\nu} + m^2 A^\nu A_\nu \quad (2.6)$$

97 where $F_{\mu\nu}$, is the field strength tensor, defined as $F_{\mu\nu} = \partial_\mu A_\nu - \partial_\nu A_\mu$

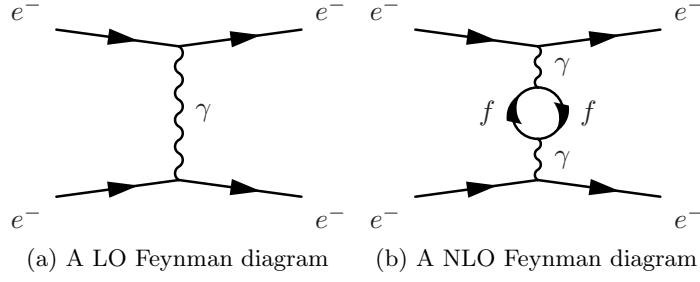


Figure 2.1: Leading and Next to Leading Order Feynman diagrams for the coulomb scattering process

Interactions are generated by coupling multiple fields together in a single term, such as $ieA_\mu\bar{\psi}\psi$ and treating it as a perturbation to the free field theory. This implies every interaction between particles is carried out by a virtual mediating particle. When two electrons scatter off one another, they are really exchanging a virtual photon, the mediator of the electromagnetic force. The W^\pm and Z bosons mediate the weak force, while the *gluons* mediate the strong force.

$$\mathcal{L} = \mathcal{L}_{Free} + \mathcal{L}_{Interacting} \quad (2.7)$$

In order to calculate the probability and dynamics of two particles interacting with one another, an integral, constrained by energy and momentum conservation, over the phase space of outgoing particles and the scattering amplitude, \mathcal{M} , is evaluated. The scattering amplitude is calculated by using the propagator (Green's function of the free particle theory) for the incoming, mediating, and outgoing particles, with an appropriate weighting function, or vertex factor, for each point the particles interact in the scattering process, and then integrating over the momentum of the mediating particle. Richard Feynmann developed a set of rules for the writing down the propagators and vertex factors directly from the Lagrangian, and easily computing the scattering amplitude. He also introduced an elegant pictographic notation useful for visualizing particle interactions, known as Feynmann diagrams.

With these tools, one can calculate the probability amplitudes of a given process occurring to Leading Order (LO) without any difficulties. However, when calculations in Next to Leading Order (NLO) are performed, and loop diagrams of virtual particles are considered, the probability amplitudes associated with a given process diverge to infinity. This occurs when one integrates over all of the possible momentum allowed by intermediate, loops of virtual particles, which due to Heisenberg's uncertainty principle, are allowed to take on any value of momentum. Figure 2.1 shows an example of a LO and NLO process.

The systematic removal of divergences from a theory is called renormalization. The divergences are absorbed into the definitions of the free parameters of the theory, making the parameters a function of the energy scale the process occurs at, instead of a constant. This

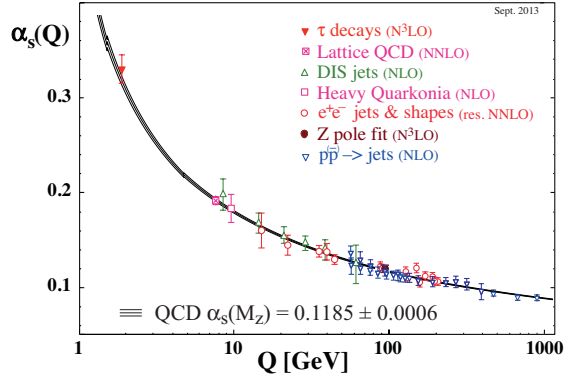


Figure 2.2: The global average of α_s , the QCD coupling constant.

allows for the calculations of fundamental processes to completed, as long as the energy scale of the interaction is known. A modern interpretation of renormalization was provided by Kenneth Wilson [4] [5]. Instead of seeing the effects of high momentum calculations after moving to NLO in perturbation theory, one uses an effective Lagrangian, computed by integrating out shells of momentum beginning at the energy cutoff of the theory, where the NLO effects begin the dominate. The dimensions of integration are then rescaled and the result of evaluating the integral over the momentum shell is absorbed into the definition of free parameters. The processes is iterated until the energy scale of the interaction is reached. The functional dependence of the parameters is then directly present in the resulting effective Lagrangian, instead of appearing suddenly when accounting for the one-loop contributions at NLO. Regardless of how strange this procedure seem, the running of the coupling constant as a function of interaction energy has been validated experimentally time and time and again, as shown in Figure 2.2 [6].

2.2 Abelian Gauge Theories of Particle Interactions

In 1930, Herman Weyl introduced the idea that the interactions between fields can be generated by requiring them to be invariant under guage transformations of a local symmetry [7]. For electromagnetism, the local symmetry is that of the Lie group, $U(1)$. It is an abelian group, which has the property that the generators of the group symmetry commutes with themselves. The $U(1)$ symmetry is invariant under phase rotations. By requiring local guage invariance, the Lagrangian must be unchanged under the

$$\psi(x) \rightarrow e^{i\alpha(x)}\psi(x). \quad (2.8)$$

Consider the Lagrangian for a free spin 1/2 particle:

$$\mathcal{L} = \bar{\psi}(i\gamma^\mu \partial_\mu - m)\psi \quad (2.9)$$

143 The first term in the Lagrangian, involving the derivative, acts on $\alpha(x)$, creating a new term in
 144 the Lagrangian, breaking its invariance under the local phase transformation.

$$\mathcal{L} \rightarrow \mathcal{L} - (\partial_\mu \alpha) \bar{\psi} \gamma^\mu \psi \quad (2.10)$$

145 Thus, a new term must be added to the original Lagrangian to cancel out the term arising from
 146 the local phase transformation. This is achieved by defining the covariant derivative:

$$D_\mu = \partial_\mu + ieA_\mu \quad (2.11)$$

147 where A_μ is a new vector field that transforms as follows:

$$A_\mu(x) \rightarrow A_\mu(x) - \frac{1}{e} \partial_\mu \alpha(x) \quad (2.12)$$

148 The covariant derivative thus transforms like

$$\begin{aligned} D_\mu \psi(x) &\rightarrow [\partial_\mu + ie(A_\mu - \frac{1}{e} \partial_\mu \alpha)] e^{i\alpha(x)} D_\mu \psi(x) \\ &= e^{i\alpha(x)} [\partial_\mu + ie(A_\mu - \frac{1}{e} \partial_\mu \alpha + \frac{1}{e} \partial_\mu \alpha)] D_\mu \psi(x) \\ &= e^{i\alpha(x)} (\partial_\mu + ieA_\mu) \psi(x) \\ &= e^{i\alpha(x)} D_\mu \psi(x) \end{aligned} \quad (2.13)$$

149 This covariant derivative transforms in the same way that $\psi(x)$ does, and the new locally gauge
 150 invariant Lagrangian becomes

$$\begin{aligned} \mathcal{L} &= \bar{\psi}(i\gamma^\mu D_\mu - m)\psi - \frac{1}{4} F^{\mu\nu} F_{\mu\nu} \\ &= i\bar{\psi} \gamma^\mu \partial_\mu \psi - \bar{\psi} \gamma^\mu \psi A_\mu - m\bar{\psi} \psi - \frac{1}{4} F^{\mu\nu} F_{\mu\nu} \end{aligned} \quad (2.14)$$

151 where

$$F^{\mu\nu} = (\partial^\mu A^\nu - \partial^\nu A^\mu) \quad (2.15)$$

152 and $\frac{1}{4} F^{\mu\nu} F_{\mu\nu}$ is the kinetic energy term of the Proca equation for the new vector field.

153 This new Lagrangian is identical to the QED Lagrangian, except it was derived beginning
 154 with a free Dirac theory and requiring the field to be locally gauge invariant under $U(1)$ transfor-
 155 mations. This necessitated the introduction of a new vector field, A_μ , as well as an interaction
 156 term with it. This implies that the electromagnetic force can be represented by the requirement

157 of local $U(1)$ symmetry on a free Dirac particle.

158 It should be noted, that if the photon had mass, an additional term from the Proca equation
 159 would have to be added to the Lagrangian, $m^2 A_\mu A^\mu$. This term complicates the picture since
 160 it is not invariant under local phase transformations, and cannot be compensated for through a
 161 different choice of A_μ . This implies that the bosons of a guage theory must be massless in order
 162 to preserve local guage invariance.

163 2.3 Non-Abelian Gauge Theories of Particle Interactions

164 In 1954, Yang and Mills worked to extend this idea to symmetries of different guage groups [8].
 165 Their most imortant accomplishment was developing this procedure for non-abelian groups.
 166 These are groups, where the transformation does not involve a simple variable $\alpha(x)$, but rather an
 167 entire matrix of dimension $n > 2$. These matrices do no commute with each other, and their work
 168 developed the procedure for applying local guage invariance described above to the more complex,
 169 higher dimensional symmetries, such as $SU(2)$ and $SU(3)$. Consider the case of $SU(2)$ symmetry.
 170 The theory is appropriate for describing the dynamics of two fermion fields, represented as a
 171 doublet:

$$\psi = \begin{pmatrix} \psi_1(x) \\ \psi_2(x) \end{pmatrix} \quad (2.16)$$

172 this will transform under the $SU(2)$ transformation as a two-component spinor:

$$\psi \rightarrow \exp\left(i\alpha^i \frac{\sigma_i}{2}\right) \psi \quad (2.17)$$

173 where σ^i are the Pauli matrices:

$$\sigma^1 = \begin{pmatrix} 0 & 1 \\ 1 & 0 \end{pmatrix}, \sigma^2 = \begin{pmatrix} 0 & -i \\ i & 0 \end{pmatrix}, \sigma^3 = \begin{pmatrix} 1 & 0 \\ 0 & -1 \end{pmatrix} \quad (2.18)$$

174 and have the commutation relation defined by:

$$\left[\frac{\sigma^i}{2}, \frac{\sigma^j}{2}\right] = i\epsilon^{ijk} \frac{\sigma^k}{2} \quad (2.19)$$

175 Similar to the case of the $U(1)$ Abelian symmetry, in order to form a lagrangian that is locally
 176 guage invariant, three vector fields, A_μ^i , $i = 1, 2, 3$, are introduced, and coupled to ψ through the
 177 covariant derivative:

$$D_\mu = (\partial_\mu - ig A_\mu^i \frac{\sigma^i}{2}) \quad (2.20)$$

178 to ensure that the derivative covaries with the transformation, the fields, A_μ^i will transform like:

$$A_\mu^i \frac{\sigma^i}{2} \rightarrow A_\mu^i \frac{\sigma^i}{2} + \frac{1}{g} (\partial_\mu \alpha^i) \frac{\sigma^i}{2} + i \left[\frac{\alpha^i \sigma^i}{2}, A_\mu^i \frac{\sigma^i}{2} \right] \quad (2.21)$$

179 The third term, which was absent from the abelian form of the transformation, is necessary to
 180 account for the non-commutation of the pauli matrices. This non-commutation also changes
 181 the form of the field strength tensor, $F_{\mu\nu}^i$:

$$F_{\mu\nu}^i = \partial_\mu A_\nu^i - \partial_\nu A_\mu^i + g \epsilon^{ijk} A_\mu^j A_\nu^k \quad (2.22)$$

182 The entire $SU(2)$ invariant Lagrangian can then be written as:

$$\begin{aligned} \mathcal{L}_{Yang-Mills} &= -\frac{1}{4} F_{\mu\nu}^i F^{i\mu\nu} + \bar{\psi} (i\gamma^\mu D_\mu) \psi \\ &= -\frac{1}{4} F_{\mu\nu}^i F^{i\mu\nu} + \bar{\psi} (i\gamma^\mu \partial_\mu - ig A_\mu^i \frac{\sigma^i}{2}) \psi \end{aligned} \quad (2.23)$$

183 This procedure generalizes to any continuous group of symmetries. The basic steps involve
 184 identifying the generators of the transformation:

$$\psi(x) \rightarrow e^{i\alpha^a t^a} \psi \quad (2.24)$$

185 where t^a are a set of matrices with the commutation relationship:

$$[t^a, t^b] = i f^{abc} t^c \quad (2.25)$$

186 where f^{abc} is the structure constant for the group. The covariant derivative is then defined as:

$$D_\mu = \partial_\mu - ig A_\mu^a t^a \quad (2.26)$$

187 where the fields, A_μ^a , transform like:

$$A_\mu^a \rightarrow A_\mu^a + \frac{1}{g} \partial_\mu \alpha^a + f^{abc} A_\mu^b \alpha^c \quad (2.27)$$

188 the field strength tensor is then formed as:

$$F_{\mu\nu}^a = \partial_\mu A_\nu^a - \partial_\nu A_\mu^a + f^{abc} A_\mu^b A_\nu^c \quad (2.28)$$

189 and finally, the locally, gauge invariant Lagrangian will have the form:

$$\begin{aligned}
\mathcal{L}_{\text{General, non-Abelian}} &= -\frac{1}{4}F_{\mu\nu}^a F^{a\mu\nu} + \bar{\psi}(i\gamma^\mu D_\mu)\psi \\
&= -\frac{1}{4}F_{\mu\nu}^a F^{a\mu\nu} + \bar{\psi}(i\gamma^\mu \partial_\mu - igA_\mu^a t^a)\psi
\end{aligned}
\tag{2.29}$$

In 1964, Murray Gell-Mann and Zweig independently developed a model of hadron interactions, that described the spectrum of baryons and mesons in terms of combinations of fundamental particles, which Gell-Mann named quarks [9] [10] [11]. In their model, three quarks: u, d, s formed an $SU(3)$ flavor symmetry. However, this did not explain the appearance of only two and three quark combinations, the mesons and baryons. It also could not explain the spin statistics of the baryons. The Δ^{++} , Δ^- , and Ω^- , particles all have uuu , ddd , sss quark combinations, respectively, with their spins aligned. That is to say, these baryons seem to violate the Pauli-exclusion principle since all three quarks seem to occupy the same quantum state simultaneously.

In 1964, O.W. Greenberg solved this problem by proposing that quarks also have an additional quantum number, *color*, that come in three types: red, green, blue [12]. The requirement that all stable hadrons be color neutral: either possessing equal amounts of all three colors in qqq combinations, or a $q\bar{q}$ pair sharing the same color, also explained the observation of only 2 and 3 quark combinations in experiments. These three colors form an $SU(3)$ symmetry, and is the gauge symmetry describing the interactions of quarks and leptons. This theory is known as Quantum Chromodynamics (QCD). Its derivation follows from the procedure outlined above. This group has eight generators, known as the Gell-Mann matrices, and are defined as:

$$\begin{aligned}
t^1 &= \frac{1}{2} \begin{pmatrix} 0 & 1 & 0 \\ 1 & 0 & 0 \\ 0 & 0 & 0 \end{pmatrix}, \quad t^2 = \frac{1}{2} \begin{pmatrix} 0 & -i & 0 \\ i & 0 & 0 \\ 0 & 0 & 0 \end{pmatrix}, \quad t^3 = \frac{1}{2} \begin{pmatrix} 1 & 0 & 0 \\ 0 & -1 & 0 \\ 0 & 0 & 0 \end{pmatrix} \\
t^4 &= \frac{1}{2} \begin{pmatrix} 0 & 0 & 1 \\ 0 & 0 & 0 \\ 1 & 0 & 0 \end{pmatrix}, \quad t^5 = \frac{1}{2} \begin{pmatrix} 0 & 0 & -i \\ 0 & 0 & 0 \\ i & 0 & 0 \end{pmatrix} \\
t^6 &= \frac{1}{2} \begin{pmatrix} 0 & 0 & 0 \\ 0 & 0 & 1 \\ 0 & 1 & 0 \end{pmatrix}, \quad t^7 = \frac{1}{2} \begin{pmatrix} 0 & 0 & 0 \\ 0 & 0 & -i \\ 0 & -i & 0 \end{pmatrix}, \quad t^8 = \frac{1}{2\sqrt{3}} \begin{pmatrix} 1 & 0 & 0 \\ 0 & 1 & 0 \\ 0 & 0 & -2 \end{pmatrix}
\end{aligned}
\tag{2.30}$$

and a Lagrangian defined as:

$$\begin{aligned}
\mathcal{L}_{QCD} &= -\frac{1}{4}G_{\mu\nu}^a G^{a\mu\nu} + \bar{\psi}(i\gamma^\mu D_\mu)\psi \\
&= -\frac{1}{4}G_{\mu\nu}^a G^{a\mu\nu} + \bar{\psi}(i\gamma^\mu \partial_\mu - igA_\mu^a t^a)\psi
\end{aligned}
\tag{2.31}$$

where t^a are the Gell-Mann matrices defined in equation 2.30 and the fields A_μ^a are the eight mediators of the QCD force, the *gluons*.

Like all non-abelian gauge theories, it is asymptotically free. Thus, the strength of the coupling constant, α_s , decreases as the momentum-transfer, Q in interaction increases. This allows the use of perturbation theory for high-momentum calculations, therefore allowing calculations of hadronic-processes for experimental evaluation.

The idea of local gauge invariance was successful in describing the dynamics of QED and QCD, which only contain massless gauge bosons. Theorists had long postulated that the weak force was so weak because it was being facilitated by massive bosons, but adding a mass term for a boson breaks the local gauge invariance. So, a tool was needed to reconcile the concept of local gauge invariance, which works so well for the other forces, with the prospect of the weak force being facilitated by massive gauge bosons.

2.4 The Higgs Mechanism in an Abelian Theory

In 1964 Peter Higgs introduced the idea that the gauge bosons can acquire their mass through the breaking of an underlying symmetry [13]. In other words, the natural symmetry of the Lagrangian describing a particular interaction could be different than the symmetry we observe in nature. Consider an abelian example of complex scalar field theory, coupled to itself and to an electromagnetic field [3].

$$\mathcal{L} = -\frac{1}{4}(F_{\mu\nu})^2 + |D_\mu\phi|^2 - V(\phi) \quad (2.32)$$

where $D_\mu = \partial_\mu + ieA_\mu$, is the familiar covariant derivative, and the Lagrangian is invariant under the $U(1)$ transformation as described earlier. The potential term, $V(\phi)$ has the form

$$V(\phi) = -\mu^2\phi^*\phi + \frac{\lambda}{2}(\phi^*\phi)^2 \quad (2.33)$$

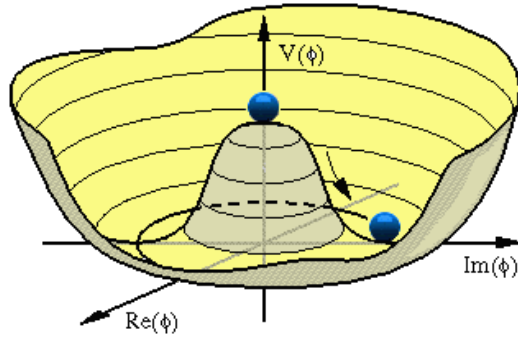


Figure 2.3: A visual representation of the Higgs potential

if $\mu^2 > 0$ the shape of the potential no longer has a minimum at $\langle\phi\rangle = 0$. Figure 2.3 shows a plot of the potential energy of ϕ in terms of each of its components. The new minimum potential energy occurs at:

$$\langle\phi\rangle = \phi_0 = \left(\frac{\mu^2}{\lambda}\right)^{1/2} \quad (2.34)$$

and while the field has a ground state at the zero potential point it is in an unstable equilibrium. Any quantum fluctuation about this point will take the field into the lower energy configuration with a ground state about the new minimum. When the Lagrangian is expanded about the field, ϕ is rewritten as:

$$\phi(x) = \phi_0 + \frac{1}{\sqrt{2}}(\phi_1(x) + i\phi_2(x)) \quad (2.35)$$

the potential term, $V(x)$, then becomes:

$$V(x) = -\frac{1}{2\lambda}\mu^4 + \frac{1}{2} \cdot 2\mu^2\phi_1^2 + \mathcal{O}(\phi_i^3) \quad (2.36)$$

where we can notice that ϕ_1 has acquired a mass term with, $m = \sqrt{2}\mu$, while the scalar field ϕ_2 remains massless, and is known as the Goldstone boson. The covariant derivative is also transformed as:

$$|D_\mu\phi|^2 = \frac{1}{2}(\partial_\mu\phi_1)^2 + \frac{1}{2}(\partial_\mu\phi_2)^2 + \sqrt{2}e\phi_0 \cdot A_\mu\partial^\mu\phi_2 + e^2\phi_0^2 A_\mu A^\mu + \dots \quad (2.37)$$

where cubic and quartic terms of A_μ , ϕ_1 , and ϕ_2 have been dropped. The important term is the last one, which can be interpreted as a mass term of the vector field, A_μ

$$\Delta\mathcal{L}_M = \frac{1}{2}m_A A_\mu A^\mu = e^2\phi_0^2 A_\mu A^\mu \quad (2.38)$$

where $m_A = 2e^2\phi_0^2$, has arisen from consequences of a non-zero vacuum expectation value of the ϕ field. The remaining, massless Goldstone boson, ϕ_2 is not a physical particle, but rather a consequence of the choice of gauge. This is illustrated when we can use the $U(1)$ gauge symmetry to rotate the field $\phi(x)$ such that the field disappears.

$$\begin{aligned} \phi &\rightarrow \phi' = e^{i\alpha}(\phi_1 + i\phi_2) \\ &= (\cos\alpha + i\sin\alpha)(\phi_1 + i\phi_2) \\ &= (\phi_1\cos\alpha - \phi_2\sin\alpha) + i(\phi_1\sin\alpha + \phi_2\cos\alpha) \\ &= (\phi_1 - \phi_2\tan\alpha) + i(\phi_1\tan\alpha + \phi_2) \end{aligned} \quad (2.39)$$

Choosing $\alpha = -\tan\phi_2/\phi_1$ will make ϕ' a real quantity and eliminate its imaginary component, ϕ'_2 . The Lagrangian can then be rewritten in terms of the rotated field ϕ' and see that massless boson is indeed removed from the theory.

$$\begin{aligned}
\mathcal{L} = & \frac{1}{2}(\partial_\mu \phi'_1)(\partial^\mu \phi'_1) - \frac{1}{2} \cdot 2\mu^2 \phi'_1 \phi'_1 \\
& - \frac{1}{4}(F^{\mu\nu} F_{\mu\nu}) + \frac{1}{2} \cdot e^2 \phi_0^2 A_\mu A^\mu \\
& + \phi_0 e^2 \phi'_1 A_\mu A^\mu + \frac{1}{2} e^2 \phi_1'^2 A_\mu A^\mu + \mathcal{O}(\phi'^3) \dots
\end{aligned} \tag{2.40}$$

The degree of freedom that ϕ_2 represents, is absorbed as a longitudinal polarization of the A_{mu} field, a forbidden for massless gauge bosons, but necessary for massive bosons.

For this case of an abelian symmetry $U(1)$, it was shown that if a complex scalar field, which interacts with itself and another vector field, can gain a non-zero vacuum expectation value. The Lagrangian can be expanded about this new minimum, generating a mass term for the vector field. One of the degrees of freedom of the original complex scalar field is then absorbed as a longitudinal polarization state of the massive vector field.

2.5 The Higgs Mechanism in a non-Abelian Theory

Before describing the electroweak gauge theory of $SU(2) \otimes U(1)$, it will be helpful to see the effects of the Higgs mechanism for the non-Abelian group, $SU(2)$ by itself. Consider an example of an $SU(2)$ gauge field coupled to a scalar field that transforms like a real-valued vector under $SU(2)$ transformations [3]. The field ϕ will have the form:

$$\phi = \begin{pmatrix} \phi_1 \\ \phi_2 \\ \phi_3 \end{pmatrix} \tag{2.41}$$

where the components, ϕ_i are real-valued fields. The $SU(2)$ transformation for this scalar field will also look like:

$$\phi \rightarrow e^{i\alpha^i T^i} \phi \tag{2.42}$$

where the matrices, T^i are defined as:

$$iT^1 = \begin{pmatrix} 0 & 0 & 0 \\ 0 & 0 & 1 \\ 0 & -1 & 0 \end{pmatrix}, \quad T^2 = \begin{pmatrix} 0 & 0 & -1 \\ 0 & 0 & 0 \\ 1 & 0 & 0 \end{pmatrix}, \quad T^3 = \begin{pmatrix} 0 & 1 & 0 \\ -1 & 0 & 0 \\ 0 & 0 & 0 \end{pmatrix} \tag{2.43}$$

The Lagrangian for this field will feature a Higgs potential term along with the previously mentioned $SU(2)$ gauge fields, A_μ^a coupled to the scalar field, ϕ , and is given by:

$$\mathcal{L} = -\frac{1}{4} F_{\mu\nu}^a F^{a\mu\nu} + |D_\mu \phi|^2 + \mu^2 \phi^* \phi - \frac{\lambda}{4} (\phi^* \phi)^2 \tag{2.44}$$

where $F_{\mu\nu}^a$, the field strength tensor is defined as:

$$F_{\mu\nu}^a = (\partial_\mu A_\nu^a - \partial_\nu A_\mu^a) + g\epsilon^{abc} A_\mu^b A_\nu^c \quad (2.45)$$

265 and the covariant derivative is defined as:

$$D_\mu = (\partial_\mu + igA_\mu^a T^a)\phi \quad (2.46)$$

266 Similarly to the Abelian case, the Higgs potential will induce a spontaneous symmetry break-
 267 ing, and one of the components of the field ϕ will gain a vacuum expectation value. After this
 268 breaking and expanding around the ground state potential, the field ϕ will have the form:

$$\phi = \frac{1}{\sqrt{2}} \begin{pmatrix} 0 \\ 0 \\ v + h \end{pmatrix} \quad (2.47)$$

269 There has been no loss in generality in assuming this form since, similarly to the abelian case,
 270 we can use the gauge symmetry of $SU(2)$ to rotate the field into this configuration. Goldstone's
 271 theorem tells us that we should expect two massive gauge bosons corresponding to the T^1 , and
 272 T^2 generators, while the T^3 generator will correspond to a massless gauge boson, since ϕ is still
 273 invariant under T^3 transformations.

274 As in the Abelian case, the mass terms for the gauge bosons are generated from the covariant
 275 derivative term, $|D_\mu \phi|^2$

$$\begin{aligned} D_\mu \phi &= \frac{1}{\sqrt{2}} \left(\partial_\mu + gA_\mu^1 \begin{pmatrix} 0 & 0 & 0 \\ 0 & 0 & 1 \\ 0 & -1 & 0 \end{pmatrix} + gA_\mu^2 \begin{pmatrix} 0 & 0 & -1 \\ 0 & 0 & 0 \\ 1 & 0 & 0 \end{pmatrix} + gA_\mu^3 \begin{pmatrix} 0 & 1 & 0 \\ -1 & 0 & 0 \\ 0 & 0 & 0 \end{pmatrix} \right) \begin{pmatrix} 0 \\ 0 \\ v + h \end{pmatrix} \\ &= \frac{1}{\sqrt{2}} \begin{pmatrix} 0 \\ 0 \\ \partial_\mu \end{pmatrix} + \frac{gA_\mu^1}{\sqrt{2}} \begin{pmatrix} 0 \\ v + h \\ 0 \end{pmatrix} - \frac{gA_\mu^2}{\sqrt{2}} \begin{pmatrix} v + h \\ 0 \\ 0 \end{pmatrix} \\ &= \frac{1}{\sqrt{2}} \begin{pmatrix} g(v + h)A_\mu^1 \\ g(v + h)A_\mu^2 \\ \partial_\mu h \end{pmatrix} \end{aligned} \quad (2.48)$$

276 Therefore

$$|D_\mu \phi|^2 = \frac{1}{2} \partial_\mu h \partial^\mu h + \frac{g^2 v^2}{2} ((A_\mu^1)^2 + (A_\mu^2)^2) + \frac{g^2}{2} (h^2 + 2hv) ((A_\mu^1)^2 + (A_\mu^2)^2) \quad (2.49)$$

This theory produces two massive bosons, A_μ^1 and A_μ^2 , both with mass, $m_A = gv$. These fields have h , and h^2 couplings to the Higgs boson. The third gauge field, A_μ^3 , remains massless and is not coupled to the Higgs field. This model is beginning to resemble a description of electroweak physics, however, a third massive boson is necessary, as is a new gauge symmetry in order to generate it. That is the subject of the next section.

2.6 Glashow Weinberg Salam Theory

Glashow, Weinberg, and Salam published their theory unifying electromagnetic and weak forces in the 1960s [14] [15] [16]. It begins with the requirement of a $SU(2)_L \otimes U(1)$ symmetry and incorporates the Higgs mechanism to give mass to the gauge bosons of the weak force. As described earlier, the $U(1)$ symmetry requires introducing a vector field, which will be labeled B_μ , and an interaction term, which is absorbed into the covariant derivative, D_μ . The transformation will also be parameterized with a quantum number, Y , known as hypercharge. The $SU(2)$ symmetry requires the introduction of three new vector fields, which will be labeled $W_\mu^i, i = 1, 2, 3$. The quantum number associated with this gauge group is known as isospin, and is determined by the T^3 operator, acting on an $SU(2)$ doublet on the third generator of the group. The $SU(2) \otimes U(1)$ transformation, $U(x)$, will then be given by:

$$U(x) = e^{i\alpha^a(x)\tau^a} e^{iY\alpha(x)/2} \quad (2.50)$$

where $\tau^a = \sigma^a/2$, the Pauli matrices, 2.18. These gauge fields will be coupled, via the covariant derivative, to a doublet of complex scalar fields ϕ , with hypercharge $Y = +1/2$. A Higgs potential will be added to generate the spontaneous symmetry breaking that will give mass to three of the gauge fields, and leave one massless. In order to preserve the $SU(2)_L \otimes U(1)$ symmetry, the new covariant derivative will take the form:

$$D_\mu = (\partial_\mu - igW_\mu^a \tau^a - \frac{i}{2}g'B_\mu) \quad (2.51)$$

The subscript L on $SU(2)_L$ refers to the experimental results that the weak force violates parity maximally, by only interacting with the left-handed chiral component of a field. Right versus left chirality is determined by whether the spin of a particle is aligned or anti-aligned with its direction of motion, and in general a particle is represented by a linear combination

of its right and left handed components. This idea was first proposed by Chen Ning Yang and Tsung-Dao Lee, in the 1950s. Their ideas were validated by the experimental discovery of parity violation in 1957, through the beta decays of Cobalt 60 atoms by C.S Wu. That same year, Yang and Lee were awarded the nobel prize for their insight [17]. In this model, then, the left-handed components of the particles participate in the weak interaction and are formed into doublets, while the right handed components are singlets, and will only interact with the electromagnetic field, B_μ . The quantum numbers of the doublet will be given by $+1/2$ for the upper component of the $SU(2)$ doublet, and $-1/2$ for the lower component. The fermion content of this theory is then given by:

$$\begin{pmatrix} \nu_L \\ e_L \end{pmatrix}, e_R \quad \begin{pmatrix} u_L \\ d_L \end{pmatrix}, u_R, d_R \quad (2.52)$$

where the right handed neutrino, ν_R has been omitted, since it has zero charge, and isospin, and therefore does not participate in any of the interactions of this theory. The complete Lagrangian is given by a sum of free particle terms for massless bosons, fermions, and Higgs scalar fields; the Higgs potential; and a Yukawa coupling term between the fermions and the Higgs, which generates their masses.

$$\mathcal{L}_{GWS} = \mathcal{L}_{BosonKE} + \mathcal{L}_{Higgs} + \mathcal{L}_{FermionKE} + \mathcal{L}_{Yukawa} \quad (2.53)$$

The Higgs potential will have the form:

$$\mathcal{L}_{Higgs} = (D_\mu \phi)^\dagger (D^\mu \phi) + \mu^2 \phi^\dagger \phi - \lambda (\phi^\dagger \phi)^2 \quad (2.54)$$

The Higgs potential will break the symmetry of the Lagrangian when one of the four degrees of freedom in the complex scalar doublet, ϕ , spontaneously acquires a vacuum expectation value. In this case, it will generate three massive gauge bosons, one massless gauge boson, and a massive scalar field. After gaining a vacuum expectation value, and expanding about this value, the scalar fields will have the form:

$$\langle \phi \rangle = \frac{1}{\sqrt{2}} \begin{pmatrix} 0 \\ v + h \end{pmatrix} \quad (2.55)$$

where no loss of generality has occurred since we are always able to rotate into this form through the appropriate gauge transformations, similar to what was described in the Abelian case. It should also be noted that this form is not invariant to any of the individual generators t^a , however ϕ will be invariant to a combination of $T^3 + Y$ generators. Per Goldstone's theorem, we

should expect this linear combination of fields to be the massless vector boson after symmetry breaking. The massless eigenstate will be the electromagnetic field, $A_\mu \sim A_\mu^3 + B_\mu$. The electric charge quantum number, Q , is then defined as

$$Q = T^3 + Y \quad (2.56)$$

321 As before, the generation of the masses for the gauge bosons are generated by the interaction
322 of their fields with the Higgs field via the covariant derivative.

$$\begin{aligned} D_\mu \phi &= \frac{1}{\sqrt{2}} \left(\partial_\mu - \frac{ig}{2} A_\mu^1 \begin{pmatrix} 0 & 1 \\ 1 & 0 \end{pmatrix} - \frac{ig}{2} A_\mu^2 \begin{pmatrix} 0 & -i \\ i & 0 \end{pmatrix} - \frac{ig}{2} A_\mu^3 \begin{pmatrix} 1 & 0 \\ 0 & -1 \end{pmatrix} \right) \begin{pmatrix} 0 \\ v+h \end{pmatrix} \\ &= \frac{1}{\sqrt{2}} \begin{pmatrix} (\frac{g}{2}(v+h)A_\mu^2) + i(\frac{g}{2}(v+h)A_\mu^1) \\ \partial_\mu + i(\frac{1}{2}(v+h)(gA_\mu^3 - g'B_\mu)) \end{pmatrix} \end{aligned} \quad (2.57)$$

323 Taking the dot product of this with its hermitian conjugate gives the $|D_\mu \phi|^2$ term:

$$\begin{aligned} |D_\mu \phi|^2 &= \frac{1}{2} \partial_\mu h \partial^\mu h + \frac{1}{2} \frac{g^2 v^2}{4} ((A_\mu^1)^2 + (A_\mu^2)^2) + \frac{v^2}{4} (gA_\mu^3 - g'B_\mu)^2 \\ &\quad + \frac{1}{2} g^2 4(h^2 + 2vh) ((A_\mu^1)^2 + (A_\mu^2)^2) + \frac{1}{2} \frac{1}{4} (h^2 + 2vh) (gA_\mu^3 - g'B_\mu)^2 \end{aligned} \quad (2.58)$$

324 From equation 2.58 we can identify three massive and one massless gauge bosons, corresponding
325 to the charged and neutral weak currents, and the electromagnetic current.

$$\begin{aligned} W_\mu^\pm &= \frac{1}{\sqrt{2}} (A_\mu^1 \mp iA_\mu^2) && \text{with mass } m_W = g \frac{v}{2}; \\ Z_\mu^0 &= \frac{1}{\sqrt{g^2 + g'^2}} (gW_\mu^3 - g'B_\mu) && \text{with mass } m_Z = \frac{v}{2} \sqrt{g^2 + g'^2}; \\ A_\mu &= \frac{1}{\sqrt{g^2 + g'^2}} (gW_\mu^3 + g'B_\mu) && \text{with mass } m_A = 0; \end{aligned} \quad (2.59)$$

326 where the last field, A_μ is absent from the covariant derivative term, but already identified as
327 the massless gauge boson of the theory due to its gauge invariance under a $T^3 + Y$ rotation.
328 Using these definitions the covariant derivative has the following form:

$$\begin{aligned} D_\mu &= \partial_\mu - \frac{ig}{\sqrt{2}} (W^+ T^+ + W^- T^-) \\ &\quad - \frac{i}{\sqrt{g^2 + g'^2}} Z_\mu^0 (gT^3 - g'Y) - \frac{gg'}{\sqrt{g^2 + g'^2}} A_\mu (T^3 + Y) \end{aligned} \quad (2.60)$$

329 where $T^\pm = \frac{1}{2}(\sigma^1 \pm \sigma^2)$. From this form, we can identify the fundamental electric charge, e , as

$$e = \frac{gg'}{\sqrt{g^2 + g'^2}} \quad (2.61)$$

330 The similarity in the forms between Z_μ^0 and A_μ suggest that their relationship can be ex-
 331 pressed in a simpler form, as the rotation of underlying guage fields A_μ^3 and B_μ through the
 332 weak mixing angle, θ_W

$$\begin{pmatrix} Z_\mu^0 \\ A_\mu \end{pmatrix} = \begin{pmatrix} \cos \theta_W & -\sin \theta_W \\ \sin \theta_W & \cos \theta_W \end{pmatrix} \begin{pmatrix} A_\mu^3 \\ B_\mu \end{pmatrix} \quad (2.62)$$

333 where $\tan \theta_W = \frac{g'}{g}$. Expanding 2.62, we have the definitions of the Z_μ^0 and A_μ fields in terms of
 334 θ_W

$$\begin{aligned} Z_\mu^0 &= A_\mu^3 \cos \theta_W - B_\mu \sin \theta_W \\ A_\mu &= A_\mu^3 \sin \theta_W + B_\mu \cos \theta_W \end{aligned} \quad (2.63)$$

335 The weak mixing angle, θ_W , also provides a simple relationship between the W_μ^\pm and Z_μ^0 fields:

$$m_W = m_Z \cos \theta_W \quad (2.64)$$

336 The covariant derivative, D_μ is also rewritten in terms of the mass eigenstates of the gauge
 337 fields

$$D_\mu = (\partial_\mu - \frac{ig}{\sqrt{2}}(W_\mu^+ + W_\mu^- T^-) - \frac{ig}{\cos \theta_W} Z_\mu^0 (T_3 - \sin^2 \theta_W Q) - ie A_\mu Q) \quad (2.65)$$

338 where $g = e / \cos \theta_W$. The square of the covariant derivative is then written as

$$\begin{aligned} |D_\mu|^2 &= \frac{1}{2} \partial_\mu h \partial^\mu h + \frac{1}{2} m_W^2 W_\mu^+ W^{\mu+} + \frac{1}{2} m_W^2 W_\mu^- W^{\mu-} + \frac{1}{2} m_Z^2 Z_\mu^0 Z^{\mu 0} \\ &\quad + (\frac{h^2}{v^2} + \frac{h}{v}) [\frac{1}{2} m_W^2 (W_\mu^+ W^{\mu+} + W_\mu^- W^{\mu-}) + \frac{1}{2} m_Z^2 Z_\mu^0 Z^{\mu 0}] \end{aligned} \quad (2.66)$$

339

340

341 With the form of the covariant derivative in place, the fermionic kinematic term of the
 342 Lagrangian can be described. As mentioned earlier, the masses of the fermions in the model
 343 will be generated by the Yukawa interaction term with the Higgs, so this term only involves the
 344 covariant derivatives acting on the left-handed doublet and right-handed singlet states of this
 345 model.

346 The quantum number assignments for the leptons, which are chosen in order to reproduce the
 347 known values of their electric charges, are shown in table 2.1. The values of these quantum

| | ν_L | e_L | e_R | u_L | d_L | u_R | d_R |
|-----------------|---------|-------|-------|-------|-------|-------|-------|
| Isospin | +1/2 | -1/2 | 0 | +1/2 | -1/2 | 0 | 0 |
| Hypercharge | -1/2 | -1/2 | -1 | +1/6 | 1/3 | 2/3 | -1/3 |
| Electric Charge | 0 | -1 | -1 | 2/3 | -1/3 | 2/3 | -1/3 |

Table 2.1: The quantum numbers Isospin and Hypercharge are assigned for each of the $SU(2)$ and $U(1)$ symmetries respectively

348 numbers enter into the covariant derivative via the Z_μ^0 term of equation 2.65. The fermionic
349 kinetic energy term of the Lagrangian is given by:

$$\begin{aligned}\mathcal{L}_{Fermion} = & \bar{E}_L(i\gamma^\mu D_\mu)E_L + \bar{e}_R(i\gamma^\mu D_\mu)e_R \\ & \bar{Q}_L(i\gamma^\mu D_\mu)Q_L + \bar{u}_R(i\gamma^\mu D_\mu)u_R + \bar{d}_R(i\gamma^\mu D_\mu)d_R\end{aligned}\quad (2.67)$$

350 Expanding the covariant term for the left-handed electron shows its explicit coupling to the
351 guage boson fields.

$$\begin{aligned}\mathcal{L}_{E_L} = & \begin{pmatrix} \bar{\nu}_L & \bar{e}_L \end{pmatrix} \left((i\gamma^\mu(\partial_\mu - \frac{ig}{\sqrt{2}}(W_\mu^+ T^+ + W_\mu^- T^-) - \frac{ig}{\cos\theta_W} Z_\mu^0(T^3 - \sin^2\theta_W Q) - ieA_\mu Q)) \right) \begin{pmatrix} \nu_L \\ e_L \end{pmatrix} \\ = & \bar{\nu}_L i\gamma^\mu \partial_\mu \nu_L + \bar{e}_L i\gamma^\mu \partial_\mu e_L + \frac{ig}{\sqrt{2}} W_\mu^+ \bar{\nu}_L \gamma^\mu e + \frac{ig}{\sqrt{2}} W_\mu^- \bar{e}_L \gamma^\mu \nu_L \\ & + \frac{ig}{\cos\theta_W} \bar{\nu}_L (1/2) \gamma^\mu \nu_L + \frac{ig}{\cos\theta_W} \bar{e}_L \gamma^\mu (-1/2 + \sin^2\theta_W(+1)) e_L + (ie) \bar{e}_L \gamma^\mu A_\mu (-1)\end{aligned}\quad (2.68)$$

352 All of the terms will be combined with the final, spontaneously broken GWS Lagranian at the
353 end of this section.

354 The final term to discuss in the theory, before combing all of the results, is the Yukawa
355 interaction term between the fermion fields and the Higgs. For the electron, this term takes the
356 form:

$$\begin{aligned}\mathcal{L}_{Yukawa} = & -\lambda_e \bar{E}_L \cdot \phi e_R - \lambda_e \bar{e}_L \cdot \phi e_R \\ = & -\frac{\lambda_e}{\sqrt{2}}(v+h)(\bar{e}_L e_R + e_L \bar{e}_R) \\ = & -\frac{\lambda_e v}{\sqrt{2}}(\bar{e}_L e_R + e_L \bar{e}_R) - \frac{\lambda_e}{\sqrt{2}}(\bar{e}_L e_R + e_L \bar{e}_R)h\end{aligned}\quad (2.69)$$

357 where the mass of the electron is identified as $m_e = \frac{\lambda_e v}{\sqrt{2}}$. In order to generate the masses of
358 the particles, each fermion has its own unique λ value. So while the Higgs mechanism is able
359 to generate the masses in a way that preserves the underlying $SU(2) \otimes U(1)$ symmetry, it does
360 not explain the heirarchy of masses since each λ value is unique to each lepton. The second
361 term in last equation of 2.69 is the coupling of the Higgs particle, h , to the fermions. The
362 coupling is proportional to the mass of the particle. The largest of these is to the top quark,

363 with $m_t = 73.21 \pm 0.51 \pm 0.71 \text{ GeV}$.

364 The Yukawa coupling for the quarks is necessarily modified when additional quarks besides
 365 the u and d are added to the theory. This is because there can be additional coupling terms
 366 that mix generations. This occurs when the mass eigenstate of the quarks is not the same as the
 367 interaction eigenstate. The modification requires the expansion of the u_L and d_L components
 368 into a vector of left handed quarks. If we let

$$u_L^i = (u_L, c_L, t_L), \quad d_L^i = (d_L, s_L, b_L) \quad (2.70)$$

369 represent the up and down-type quarks in the original weak interaction basis, then the vectors,
 370 u_L^i and d_L^i , can be defined as the diagonalized basis for the Higgs coupling. They are related
 371 through a unitary transformation.

$$u_L^i = U_u^{ij} u_L^{j'}, \quad d_L^i = U_d^{ij} d_L^{j'} \quad (2.71)$$

372 The interaction terms with the charged gauge boson currents must then be rewritten as

$$J_W^{\mu+} = \frac{1}{\sqrt{2}} \bar{u}_L^i \gamma^\mu d_L^i = \frac{1}{\sqrt{2}} \bar{u}_L^{i'} \gamma^\mu (U_u^\dagger U_d) d_L^{j'} = \frac{1}{\sqrt{2}} \bar{u}_L^{i'} \gamma^\mu V_{ij} d_L^{j'} \quad (2.72)$$

373 where V_{ij} is the 3x3 Cobibbo-Kobayashi-Maskawa (CKM) matrix describing the mixing among
 374 six quarks [18] [19]. It is an extension of the Glashow-Iliopoulos-Maiaini mechanism, which
 375 was a 2x2 matrix that predicted the existence of a fourth quark, the charm quark. The GIM
 376 mechanism was an attempt to suppress flavor-changing-neutral currents, which occur at LO in
 377 a three-quark model, but not in a four-quark model. The CKM matrix, however, was motivated
 378 by an attempt to explain CP violation in the weak interaction. At the time of its publication,
 379 the bottom and top quarks were not predicted. After these were discovered, they were awarded
 380 the nobel prize in physics in 2008.

381 At this point, all the of the pieces are ready to write down the GWS Lagrangian, after the
 382 Higgs mechanism has spontaneously broken the $SU(2) \otimes U(1)$ symmetry.

$$\begin{aligned} \mathcal{L}_{Unbroken} = & -\frac{1}{4} A_{\mu\nu}^a A^{\mu\nu a} - \frac{1}{4} F_{\mu\nu} F^{\mu\nu} \\ & + |D_\mu \phi|^2 + \mu^2 (\phi^\dagger \phi) - \lambda (\phi^\dagger \phi)^2 \\ & + \bar{E}_L (i \gamma^\mu D_\mu) E_L + \text{similar terms for } e_R, U_L, u_R, d_R \\ & - \lambda_e \bar{E}_L \cdot \phi e_R + h.c. + \text{similar terms for } e_R, U_L, u_R, d_R \end{aligned} \quad (2.73)$$

$$\begin{aligned}
\mathcal{L}_{GWS} = & -\frac{1}{4}(Z_{\mu\nu}^0)^2 - \frac{1}{2}(W_{\mu\nu}^+ W_{\mu\nu}^-) - \frac{1}{4}(F_{\mu\nu})^2 \\
& + ig \cos \theta_W ((W_\mu^- W_\nu^+ - W_\nu^- W_\mu^+) \partial^\mu Z^{0\nu} + W_{\mu\nu}^+ W^{-\mu} Z^{0\nu} + W_{\mu\nu}^- W^{+\mu} Z^{0\nu}) \\
& + ie ((W_\mu^- W_\nu^+ - W_\nu^- W_\mu^+) \partial^\mu A^\nu + W_{\mu\nu}^+ W^{-\mu} A^\nu - W_{\mu\nu}^- W^{+\mu} A^\nu) \\
& + g^2 \cos^2 \theta_W (W_\mu^+ W_\nu^- Z^{0\mu} Z^{0\nu} - W_\mu^+ W^{-\mu} Z_\nu^0 Z^{0\nu}) \\
& + g^2 (W_\mu^+ W_\mu^- A^\mu A^\nu - W_\mu^+ W^{-\mu} A_\nu A^\nu) \\
& + ge \cos \theta_W (W_\mu^+ W_\nu^- (Z^{0\mu} A_\nu + Z^{0\nu} A^\mu) - 2W_\mu^+ W^{-\mu} A^\nu) \\
& + \frac{1}{2} g^2 (W_\mu^+ W_\nu^-) (W^{+\mu} W^{-\nu} - W^{+\nu} W^{-\mu}) \\
& + \frac{1}{2} \partial_\mu h \partial^\nu h - v^2 \lambda h^2 + \frac{1}{2} m_W^2 W_\mu^+ W^{+\mu} + \frac{1}{2} m_W^2 W_\mu^- W^{-\mu} + \frac{1}{2} m_Z^2 Z_\mu^0 Z^{0\mu} \\
& + \left(\frac{h^2}{v^2} + \frac{h}{v} \right) \left(\frac{1}{2} m_W^2 (W_\mu^+ W^{+\mu} + W_\mu^- W^{-\mu}) + \frac{1}{2} m_Z^2 Z_\mu^0 Z^{0\mu} \right) - \lambda v h^3 - \frac{1}{4} \lambda h^4 \\
& + \bar{E}_L (i\gamma^\mu \partial_\mu) E_L + \bar{e}_R (i\gamma^\mu \partial_\mu) e_R + \bar{Q}_L (i\gamma^\mu \partial_\mu) Q_L + \bar{u}_R (i\gamma^\mu \partial_\mu) u_R + \bar{d}_R (i\gamma^\mu \partial_\mu) d_R \\
& + g(W_\mu^+ J_W^{\mu+} + W_\mu^- J_W^{\mu-} + Z_\mu^0 J_Z^\mu) + e A_\mu J_{EM}^\mu \\
& - \frac{\lambda_e v}{\sqrt{2}} (\bar{e}_L e_R + \bar{e}_R e_L) + -\frac{\lambda_e h}{\sqrt{2}} (\bar{e}_L e_R + \bar{e}_R e_L) \\
& - \frac{\lambda_u v}{\sqrt{2}} (\bar{u}_L u_R + \bar{u}_R u_L) + -\frac{\lambda_u h}{\sqrt{2}} (\bar{u}_L u_R + \bar{u}_R u_L) \\
& - \frac{\lambda_d v}{\sqrt{2}} (\bar{d}_L d_R + \bar{d}_R d_L) + -\frac{\lambda_d h}{\sqrt{2}} (\bar{d}_L d_R + \bar{d}_R d_L)
\end{aligned} \tag{2.74}$$

where the currents of the electroweak interaction, $J_W^{\mu+}$, $J_W^{\mu-}$, J_Z^μ , J_A^μ are defined as:

$$\begin{aligned}
J_W^{\mu+} &= \frac{1}{\sqrt{2}} \left(\bar{\nu}_L \gamma^\mu e_L + \bar{u}_L' \gamma^\mu V_{ij} d_L^{j'} \right) \\
J_W^{\mu-} &= \frac{1}{\sqrt{2}} \left(\bar{e}_L \gamma^\mu \nu_L + \bar{d}_L' \gamma^\mu V_{ij} u_L^{j'} \right) \\
J_Z^\mu &= \frac{1}{\cos \theta_W} (\bar{\nu}_L \gamma^\mu (+1/2) \nu_L + \bar{e}_L \gamma^\mu (-1/2 + \sin^2 \theta_W) e_L + \bar{e}_R \gamma^\mu \sin^2 \theta_W e_R \\
&\quad + \bar{u}_L \gamma^\mu (1/2 - 2/3 \sin^2 \theta_W) u_L + \bar{u}_R \gamma^\mu (-2/3 \sin^2 \theta_W) u_R \\
&\quad + \bar{d}_L \gamma^\mu (-1/2 + 1/3 \sin^2 \theta_W) d_L + \bar{d}_R \gamma^\mu (1/3 \sin^2 \theta_W) d_R) \\
J_{EM}^\mu &= e_{L,R} \gamma^\mu (-1) e_{L,R} + u_{L,R} \gamma^\mu (2/3) u_{L,R} + d_{L,R} \gamma^\mu (-2/3) d_{L,R}
\end{aligned} \tag{2.75}$$

2.7 The Standard Model of Particle Physics

The Standard Model of particle physics, extends the GWS model by incorporating the QCD interaction between the quarks and gluons. The symmetry of this theory is that of:

$$SU(3)_C \otimes SU(2)_L \otimes U(1)_\gamma \tag{2.76}$$

384 The Lagrangian of the model is given by

$$\mathcal{L}_{SM} = \mathcal{L}_{GWS} - \frac{1}{4} G_{\mu\nu}^a G^{a\mu\nu} + g_S C_\mu^a J_{QCD}^{a\mu} \quad (2.77)$$

385 where the current for the QCD interaction, $J_{QCD}^{a\mu}$ is defined as:

$$J_{QCD}^a = \bar{u}^i \gamma^\mu t^a u^i + \bar{d}^i \gamma^\mu t^a d^i \quad (2.78)$$

386 where t^a are the Gell-Mann matrices defined in equation 2.30. The field strength tensor for the
387 eight gluon fields, $G_{\mu\nu}^a$, is defined as

$$G_{\mu\nu}^a = (\partial_\mu C_\nu^a - \partial_\nu C_\mu^a) - g_S f^{abc} C_\mu^b C_\nu^c \quad (2.79)$$

388 The experimental evidence in favor of the SM is compelling. It has not only been able
389 to describe existing phenomenon to great precision, but has also predicted the existence of
390 new forms of matter and interactions among fundamental particles. The UA1 [20] [21] and
391 UA2 [22] [23] experiments at CERN, under the leadership of Carlo Rubbia, discovered the
392 W and Z bosons in 1983. The experiments observed a handful of events, in $p\bar{p}$ collisions, at
393 $\sqrt{s} = 540 \text{ GeV}$, and were able to measure the masses to be $M_W \sim 80 \text{ GeV}$ and $M_Z \sim 95 \text{ GeV}$.

394 In the following years, from 1989-2000, the Large electron-positron (LEP) collider at CERN
395 conducted precision measurments of the Standard Model [24] [25]. Along with high-precision
396 measurements on the W, Z masses:

$$\begin{aligned} m_Z &= 91.1875 \pm 0.0021 \text{ GeV} \\ m_W &= 80.376 \pm 0.0033 \text{ GeV} \end{aligned} \quad (2.80)$$

397 the experiment was also able to put stringent limits on the existence of more than three families
398 of leptons and quarks by measuring the width of the Z boson. Figure 2.4 shows the comparison
399 of two, three, and four family hypotheses to data.

400 Another milestone for the Standard Model occured in 1995 when the CDF [26] and D0 exper-
401 iments [27] at the Tevatron announced the observation of the top quark, with $m_t \sim 176 \text{ GeV}$,
402 in $p\bar{p}$ collisions at $\sqrt{s} = 1.8 \text{ TeV}$. Figure 2.6 shows a plot from 2012, the latest top quark mass
403 measurements from CDF, which reports a $m_t = 173.18 \pm 0.56 \pm 0.75 \text{ GeV}$. It was the last quark
404 predicted by the CKM matrix to be observed, and earned Makoto Kobayashi and Toshihide
405 Maskawa the nobel prize in 2008 for their work extending the quark sector to three families and
406 parameterizing their electroweak mixing.

407 Yet another milestone was reached in 2012, when the CMS and ATLAS detectors at CERN

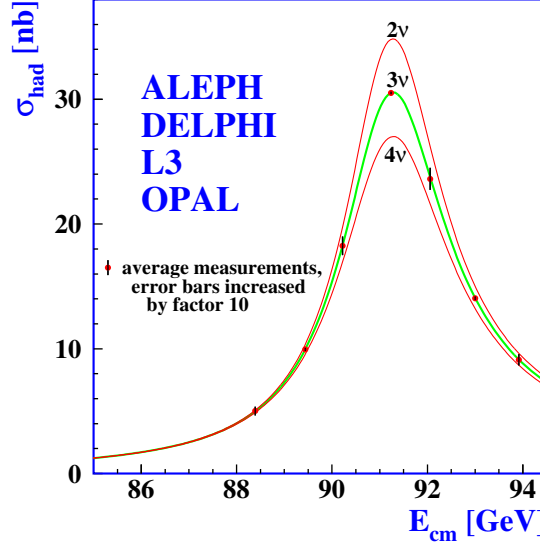


Figure 2.4: Experimental results of the width of Z boson from LEP, comparing the hypotheses of 2, 3, or 4 neutrino generations

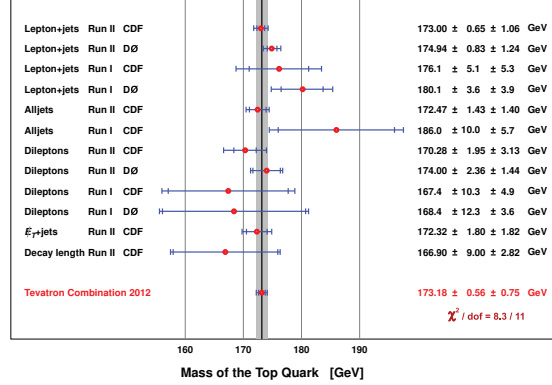


Figure 2.5: Recent experimental results of the top mass from the CDF detector at the Tevatron

announced the observation of a new boson, with characteristics strikingly similar to the elusive Higgs boson of the SM. Figure 2.6 shows the latest measurement results on the mass from the $H \rightarrow \gamma\gamma$ and $H \rightarrow ZZ$ channels, with a $m_H = 125.02 \pm 0.27 \pm 0.15$. One of the most important remaining goals is to measure the couplings of this new boson to all of the other particles in the Standard Model. Of particular interest is the coupling to the top-quark, since it offers the largest value of the Higgs Yukawa coupling to measure. This offers a test of the nature of the coupling, as well as a probe into deviations from its value.

2.8 Higgs Production in pp Collisions at the LHC

The rest of the thesis will describe the search for Higgs boson production in proton-proton collisions at the LHC, so it will be useful to understand the production mechanisms for the Higgs in this scenario. At the LHC collision energies 7 – 14 TeV, there are four dominant production

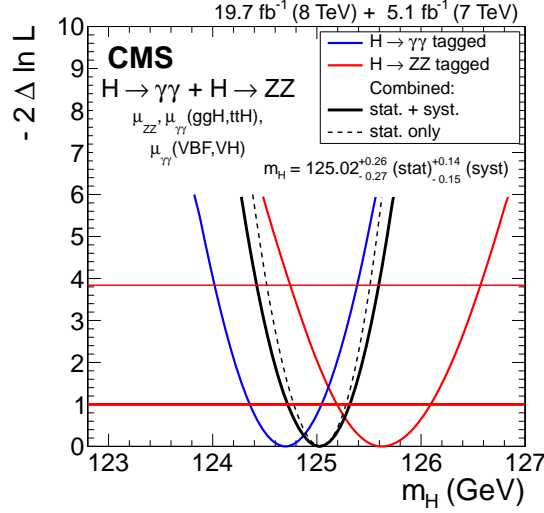
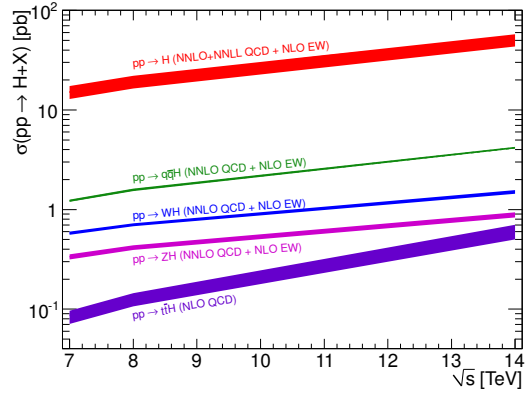


Figure 2.6: Recent experimental results of the Higgs mass from the CMS detector at the LHC


 Figure 2.7: Higgs production cross-sections at the LHC, for 7-14 TeV pp collisions

mechanisms that produce Higgs events: gluon-gluon fusion (ggf), vector-boson fusion (vbf),
 associated production with vector bosons (VH), and associated production with top-quark pairs
 ($t\bar{t}H$). Figure 2.7 shows the relative cross sections for each of these mechanisms.

Show plot of production mechanisms

Gluon-Gluon Fusion and diagram

Vector Boson Fusion and diagram

Associated Production and diagram

2.9 $t\bar{t}H$ Production and Background Processes in pp Collisions at the LHC

For this special case of pp collisions show diagram of $t\bar{t}H$ production.

backgrounds for this are dominated by $t\bar{t} + jets$ in particular $t\bar{t} + b\bar{b}$. Show diagrams

Single Top

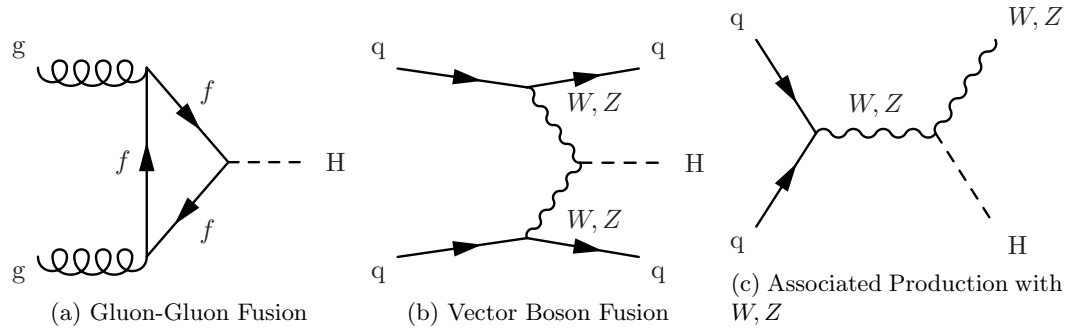


Figure 2.8: Feynman diagrams for the three largest Higgs production modes at the LHC

431 Diboson
432 W/Z jets

433 2.10 Potential BSM Effects on $t\bar{t}H$ production

434 Fourth generation
435 Vector-like top quark
436 SUSY

437 Chapter 3

438 The Large Hadron Collider

439 The Large Hadron Collider (LHC), is a proton-proton collider operated by the European Center
440 for Nuclear Research (CERN)

441 3.1 From a bottle of Hydrogen

442 Our journey begins with a bottle of Hydrogen that is Attached somewhere before being ionized
443 and zipped up to the speed of light.

444 Such humble beginnings for a tool that is to become the most powerful probe of nature
445 mankind has ever wielded.

446 3.2 Klystron

447 This is basically a giant microwave cavity that initially accelerates the protons up to some speed.

448 3.3 Something Comes Next

449 Should really know more about how protons get up to these speeds.

450 3.4 The Main Injector

451 Then the protons come here and are injected into the LHC

452 3.5 The LHC Ring

453 Big magnets, one blew up once, cryogenics, vacuum better than space. Cool.

454 **3.6 Final Structure and Beam Spacing**

455 Bunch structure, talk about important parameters of the beam

456 Chapter 4

457 The Compact Muon Solenoid

458 The Compact Muon Solenoid (CMS) is one of two general purpose detectors at the LHC.

459 4.1 The Inner Tracker

460 The inner tracker is silicon and really really big, lots of channels.

461 4.2 The Electromagnetic Calorimeter

462 PbWO₄ crystals. APDs in the Barrel. VPTs in the Endcaps

463 4.2.1 Vacuum Photo-Triodes

464 Extra time for VPTs

465 4.2.2 Test Rig at UVa

466 Big magnet, lots of light, test dem led's

467 4.2.3 Results of UVa Tests

468 Plots, Plots, plots, plots, plots

469 4.3 The Hadronic Calorimeter

470 Brass, Steel, Soviet Sweat

4.4 Forward Calorimetry

High eta, great for VBF

4.5 Magnet and Return Yoke

Describe solenoid and measuring field, and engineering marvel or return yoke structure.

4.6 Muon Chambers

APDs DTs and CSCs

4.7 Data Collection Overview

L1 trigger, HLT etc

Chapter 5

Particle Reconstruction at CMS

Data is reconstructed at CMS using the *ParticleFlow*TM algorithm

5.1 Muon Reconstruction

Muons rely heavily on the inner tracker and muons chambers for efficient identification and reconstruction

5.2 Electron Reconstruction

Electrons leave charged tracks in the inner tracker, and create a wide shower of particles and thus energy deposits in the ECAL. High energy electrons sometimes traverse the entire distance of the ECAL and leave energy in the HCAL, however the ratio of these two energies is disproportionate for the ECAL, and thus this ratio is often used to discriminate electrons from highly electromagnetic hadronic jets.

5.3 Photon Reconstruction

Like electrons, but with no tracks, and narrower shower shape.

5.4 Jet Reconstruction

Jets are formed by matching tracks from the inner tracker to energy deposits in the ECAL and HCAL. Energy clusters are identified from the ECAL and HCAL, and everything is then clustered in a cone.

5.5 Tau Reconstruction

So heavy that they decay to leptons or hadrons before traversing the detector, they still leave an oddly-numbered pronged decay hadronically due to charge conservation requiring that one of the hadrons produced be equal charge to the tau. This results in one charged, and any number of neutral pions, or three charged, and any number of neutral pions.

5.6 Missing Transverse Energy Reconstruction

since the detector is hermetic, and the tracker so granular, we can ensure that no particles flew out of the detector due to lack of coverage. Only long-lived neutral particles can escape, such as neutrinos in the standard model. Many BSM theories, such as SUSY, are characterized by stable, neutral particles.

MET is the vector sum of all of the tracks associated with a particular primary vertex (? or all vertices in event). Thus if there was a neutral particle that escaped detection, there would be a momentum imbalance along the trajectory of that particle. This is how neutrinos are identified.

Bibliography

- [1] CMS Collaboration, “Observation of a new boson at a mass of 125 GeV with the CMS experiment at the LHC”, *Phys.Lett.B* (2012) [arXiv:1207.7235](#).
- [2] ATLAS Collaboration, “Observation of a new particle in the search for the Standard Model Higgs boson with the ATLAS detector at the LHC”, *Phys.Lett.B* (2012) [arXiv:1207.7214](#).
- [3] M. E. Peskin and D. V. Schroeder, “An Introduction to Quantum Field Theory”. Westview Press, URL <http://www.westviewpress.com>, 1995.
- [4] K. G. Wilson, “Renormalization Group and Critical Phenomena. I. Renormalization Group and the Kadanoff Scaling Picture”, *Phys. Rev. B* **4** (Nov, 1971) 3174–3183, [doi:10.1103/PhysRevB.4.3174](#).
- [5] K. G. Wilson, “Renormalization Group and Critical Phenomena. II. Phase-Space Cell Analysis of Critical Behavior”, *Phys. Rev. B* **4** (Nov, 1971) 3184–3205, [doi:10.1103/PhysRevB.4.3184](#).
- [6] S. Bethke, “The 2009 World Average of $\alpha(s)$ ”, *Eur.Phys.J.* **C64** (2009) 689–703, [doi:10.1140/epjc/s10052-009-1173-1](#), [arXiv:0908.1135](#).
- [7] H. Weyl, “The theory of groups and quantum mechanics”. Dover Press, URL <https://ia700807.us.archive.org/20/items/ost-chemistry-quantumtheoryofa029235mbp/quantumtheoryofa029235mbp.pdf>, 1930.
- [8] C. N. Yang and R. L. Mills, “Conservation of Isotopic Spin and Isotopic Gauge Invariance”, *Phys. Rev.* **96** (Oct, 1954) 191–195, [doi:10.1103/PhysRev.96.191](#).
- [9] M. Gell-Mann, “A Schematic Model of Baryons and Mesons”, *Phys.Lett.* **8** (1964) 214–215, [doi:10.1016/S0031-9163\(64\)92001-3](#).
- [10] G. Zweig, “An SU_3 model for strong interaction symmetry and its breaking; Version 1”, Technical Report CERN-TH-401, CERN, Geneva, Jan, 1964.

- [11] G. Zweig, “An SU_3 model for strong interaction symmetry and its breaking; Version 2”,.
- [12] O. W. Greenberg, “Spin and Unitary-Spin Independence in a Paraquark Model of Baryons and Mesons”, *Phys. Rev. Lett.* **13** (Nov, 1964) 598–602,
doi:[10.1103/PhysRevLett.13.598](https://doi.org/10.1103/PhysRevLett.13.598).
- [13] P. Higgs, “Broken symmetries, massless particles and gauge fields”, *Physics Letters* **12** (1964), no. 2, 132 – 133, doi:[http://dx.doi.org/10.1016/0031-9163\(64\)91136-9](http://dx.doi.org/10.1016/0031-9163(64)91136-9).
- [14] S. Weinberg, “A Model of Leptons”, *Phys. Rev. Lett.* **19** (Nov, 1967) 1264–1266,
doi:[10.1103/PhysRevLett.19.1264](https://doi.org/10.1103/PhysRevLett.19.1264).
- [15] S. L. Glashow, “Partial-symmetries of weak interactions”, *Nuclear Physics* **22** (1961), no. 4, 579 – 588, doi:[http://dx.doi.org/10.1016/0029-5582\(61\)90469-2](http://dx.doi.org/10.1016/0029-5582(61)90469-2).
- [16] A. Salam and J. Ward, “Electromagnetic and weak interactions”, *Physics Letters* **13** (1964), no. 2, 168 – 171, doi:[http://dx.doi.org/10.1016/0031-9163\(64\)90711-5](http://dx.doi.org/10.1016/0031-9163(64)90711-5).
- [17] Nobelprize.org, “The Nobel Prize in Physics 1957”.
URL http://www.nobelprize.org/nobel_prizes/physics/laureates/1957/.
- [18] N. Cabibbo, “Unitary Symmetry and Leptonic Decays”, *Phys. Rev. Lett.* **10** (Jun, 1963) 531–533, doi:[10.1103/PhysRevLett.10.531](https://doi.org/10.1103/PhysRevLett.10.531).
- [19] M. Kobayashi and T. Maskawa, “CP Violation in the Renormalizable Theory of Weak Interaction”, *Prog.Theor.Phys.* **49** (1973) 652–657, doi:[10.1143/PTP.49.652](https://doi.org/10.1143/PTP.49.652).
- [20] G. Arnison et al., “Experimental observation of isolated large transverse energy electrons with associated missing energy at $s=540$ GeV”, *Physics Letters B* **122** (1983), no. 1, 103 – 116, doi:[http://dx.doi.org/10.1016/0370-2693\(83\)91177-2](http://dx.doi.org/10.1016/0370-2693(83)91177-2).
- [21] G. Arnison et al., “Experimental observation of lepton pairs of invariant mass around 95 GeV/ c^2 at the {CERN} {SPS} collider”, *Physics Letters B* **126** (1983), no. 5, 398 – 410,
doi:[http://dx.doi.org/10.1016/0370-2693\(83\)90188-0](http://dx.doi.org/10.1016/0370-2693(83)90188-0).
- [22] M. Banner et al., “Observation of single isolated electrons of high transverse momentum in events with missing transverse energy at the {CERN} pp collider”, *Physics Letters B* **122** (1983), no. 56, 476 – 485,
doi:[http://dx.doi.org/10.1016/0370-2693\(83\)91605-2](http://dx.doi.org/10.1016/0370-2693(83)91605-2).
- [23] P. Bagnaia et al., “Evidence for $Z^0 e^+ e^-$ at the {CERN} pp collider”, *Physics Letters B* **129** (1983), no. 12, 130 – 140,
doi:[http://dx.doi.org/10.1016/0370-2693\(83\)90744-X](http://dx.doi.org/10.1016/0370-2693(83)90744-X).

- [24] The ALEPH, DELPHI, L3, OPAL, SLD Collaborations, the LEP Electroweak Working Group, the SLD Electroweak and Heavy Flavour Groups, “Precision Electroweak Measurements on the Z Resonance”, *Phys. Rept.* **427** (2006) 257, [arXiv:hep-ex/0509008](#).
- [25] The ALEPH, DELPHI, L3, OPAL Collaborations, the LEP Electroweak Working Group, “Electroweak Measurements in Electron-Positron Collisions at W-Boson-Pair Energies at LEP”, *Phys. Rept.* **532** (2013) 119, [arXiv:1302.3415](#).
- [26] F. Abe et al., “Observation of Top Quark Production in $\bar{p}p$ Collisions with the Collider Detector at Fermilab”, *Phys. Rev. Lett.* **74** (Apr, 1995) 2626–2631, [doi:10.1103/PhysRevLett.74.2626](#).
- [27] S. Abachi et al., “Search for High Mass Top Quark Production in $p\bar{p}$ Collisions at $\sqrt{s} = 1.8$ TeV”, *Phys. Rev. Lett.* **74** (Mar, 1995) 2422–2426, [doi:10.1103/PhysRevLett.74.2422](#).

579 List of Acryonyms

580 **ATLAS** A Toroidal LHC Apparatus

581 **BSM** Beyond the Standard Model

582 **CERN** European Center for Nuclear Research

583 **CMS** Compact Muon Solenoid

584 **FSR** Final State Radiation

585 **ISR** Initial State Radiation

586 **JHEP** Journal of High Energy Physics

587 **LHC** Large Hadron Collider

588 **LO** Leading Order

589 **MVA** Multi-Variate Analysis

590 **NLO** Next to Leading Order

591 **QCD** Quantum Chromodynamics

592 **QED** Quantum Electrodynamics

593 **QFT** Quantum Field Theory

594 **SM** Standard Model